PHYSICAL REVIEW B VOLUME 50, NUMBER 23 15 DECEMBER 1994-I

Quantum magnetotransport of electrons in double-barrier resonant-tunneling structures

Guo Yong
Department of Physics, Hebei Teachers' University, 050016, People's Republic of China

You-Cheng Li, Xiao-Jun Kong, and Cheng-Wen Wei
China Center of Advanced Science and Technology (World Laboratory), P.O. Box 8730, Beijing 100080, China;
National Laboratory for Superlattices and Microstructures, P.O. Box 912, Beijing, China;
and Department of Physics, Hebei Teachers' University, 050016, People's Republic of China
(Received 5 January 1994; revised manuscript received 15 July 1994)

In this paper, the one-dimensional effective-mass equation is solved analytically by means of Hermitian functions as envelope functions under crossed magnetic and electric fields. By using the transfer-matrix method, we calculate the transmission coefficient for electrons tunneling through several different double-barrier resonant-tunneling structures (DBRTS's). It is found that, for DBRTS's with higher barriers and thinner width, the peak transmission coefficient P_m is nearly equal to unity and is not off unity until the magnetic field **B** becomes much stronger. However, for DBRTS's with much lower barriers and thicker width, P_m is far off unity even when **B** is small. With the bias increasing, for a constant **B**, the resonant-tunneling peaks will shift to lower energy, and after reaching the unity value, the value of P_m will decrease up to the disappearance of the peak. The J-V characteristics of DBRTS's are also presented in which the peak markedly decreases and shifts to higher bias when **B** is increased.

I. INTRODUCTION

Superlattices, especially semiconductor-based superlattices, have great potential in minimizing semiconductor devices and improving their speed. Double-barrier resonant-tunneling structures (DBRTS's) have found wide applications in many new devices, such as photodetectors, diodes, transistors, low-power logic circuits, and quantum integrated circuits, etc. In the early 1970s Esaki and Tsu[1] realized the theoretical significance of both the resonant tunneling and negative differential conductance. Since the larger ratio between peaks and valleys was observed experimentally by Sollner *et al.*,[2] the resonant tunneling through superlattices has attracted considerable interest and has been widely investigated theoretically and experimentally.

Recently, magnetotunneling has proven to be a powerful tool to study the dynamics of electrons in DBRTS's. Magnetotunneling in a parallel field $\mathbf{B}_{\parallel}$ ($\mathbf{B}\parallel\mathbf{J}$) has been studied by a number of researchers,[3–7] the tunneling Hamiltonian in this case is separable and the transport along the tunneling direction is independent of transverse momentum. The observed magnetotunneling steps can be clearly associated with the alignment of Landau levels in the emitter and the well. For the transverse field $\mathbf{B}_{\perp}$, the situation is more complex, as the confinement by the magnetic field mixes with the heterostructure double-barrier potential in the tunneling direction and the transport along the tunneling direction no longer conserves all the transverse-momentum components. Experimentally, it has been found that a transverse magnetic field weakens the features in the J-V characteristics and shifts them to higher voltages.[8–16] This has been explained qualitatively by the change in transverse momentum suffered by an electron tunneling in a transverse magnetic field.

A number of researchers have studied the transverse magnetotunneling theoretically. By using the WKB approximation, Ancilotto[17] investigated the effect of a transverse magnetic field and gave a direct numerical solution of the one-dimensional effective-mass equation. Cruz, Hernandez-Cabrera, and Aceituno[18] solved the same equation analytically by means of the confluent hypergeometric functions as envelope functions and calculated the transmission coefficient for tunneling through double barriers and superlattices of $GaAs/Ga_{1-x}Al_xAs$ in an applied transverse-magnetic field. They all found that the value of the transmission coefficient at resonance is not affected by the presence of the magnetic field but the overall shape of the transmission coefficient reflects the reduction in current along the heterostructure axis due to the Lorentz force. In their calculations, the following assumptions have been made: (i) The effective-mass approximation is valid and electrons are described by quadratic energy-momentum relations. (ii) The electron free path is larger than the size of the double-barrier structure. (iii) The magnetic field is confined to the barrier region. (iv) The effects of phonon scattering are negligible. (v) The effects of space charge are also ignored in which accumulation and depletion layers may form and the charge buildup in the well may be created.

In this paper, under crossed magnetic and electric fields the one-dimensional effective-mass equation is solved analytically by using Hermitian functions as envelope functions. We calculate the transmission coefficient $P(E,V,B,k_y)$ for the electron tunneling through several different types of DBRTS's by means of the transfer-matrix method. In our calculations, we make the following considerations: (i) using different electron effective masses inside the well and barriers separately; (ii) imposing strict continuity of the wave function

Ψ and its appropriately normalized derivative $(1/m^*)(d\Psi/dz)$ at the boundary; and (iii) considering the voltage to drop nonuniformly across the device. Without the bias applied, it is found that for DBRTS's with higher barriers and thinner width, the peak transmission coefficient P_m at resonance is nearly equal to unity and is not off unity until the magnetic field becomes very strong; but for DBRTS's with much lower barriers and thicker width, P_m is far off unity even when B is not much stronger. It is also found that with increasing magnetic field, the resonant peaks of $P(E,V,B,k_y)$ become narrow and shift to higher energies. When the bias is applied and the magnetic field is taken as a constant, the resonant-tunneling peaks will shift to lower energies with increasing bias. In this case, at the outset P_m increases slightly and when P_m reaches nearly unity value, it begins to decrease until the peak disappears. The J-V characteristics of DBRTS's under crossed electric and magnetic fields is also presented.

The organization of the rest of this paper is as follows. In Sec. II, we describe the transfer-matrix approach of quantum magnetotunneling. In Sec. III, we present our calculated results on the transmission coefficients and tunneling current. In Sec. IV, we give a brief summary.

II. TRANSFER-MATRIX THEORY OF QUANTUM MAGNETOTUNNELING

We assume the GaAs/Al_xGa_{1-x}As heterostructure placed in crossed electric and magnetic fields with its growth direction along the z axis. The electric field F is directed along the z axis; the magnetic field $\mathbf{B}$ is taken to be uniform and directed along the positive x direction.

Let us consider a beam of particles with kinetic energy E and effective mass m_i^* to be incident on a DBRTS. Figure 1 shows the DBRTS potential profile under a positive bias V for the case $B=0$. For simplicity, both fields are supposed to vanish outside the device region $[0,a]$. We choose the Landau gauge associated with the magnetic field as $A=(0,-Bz,0)$, where B is the magnetic-field strength. The conduction-band offset U_0, effective mass m_i^*, and the dielectric constant ϵ_i in each region of the GaAs/Al_xGa_{1-x}As DBRTS's are determined as functions of the aluminum concentration x by the following standard approximations:[19]

$$U_0=\begin{cases}0.75x\ \text{eV}\quad (0\le x\le 0.45)\\ 0.75x+0.69(x-0.45)^2\ \text{eV}\quad (0.45\le x\le 1)\ ,\end{cases} \tag{1}$$

$$m_i^*/m_e=0.067+0.083x\quad (0\le x\le 1)\ , \tag{2}$$

$$\epsilon_i/\epsilon_0=13.1-3.0x\quad (0\le x\le 1)\ , \tag{3}$$

where m_e is the free-electron mass, ϵ_0 is the dielectric constant in a vacuum. For all the equations in this paper, subscript and superscript i represent the different regions of the DBRTS, i.e., $i=1,2,3,4,5$ correspond to regions I, II, III, IV, and V.

The Hamiltonian of an electron in each region in the DBRTS is given by

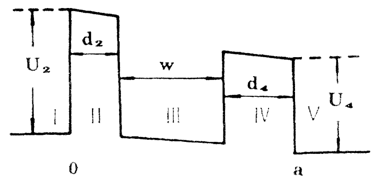

FIG. 1. Potential-energy diagram of the DBRTS with an applied voltage.

$$H=(P_x^2+P_y^2+P_z^2)/(2m_i^*)\quad (i=1,z<0)\ , \tag{4}$$

$$H=[P_x^2+(P_y+eBz)^2+P_z^2]/2m_i^*+U_i(z)$$
$$-\begin{cases}eF_iz\quad (i=2,\ 0<z<d_2)\\ eF_2d_2+eF_i(z-d_2)\quad (i=3,\ d_2\le z\le d_2+w)\\ eF_2d_2+eF_3w+eF_i(z-d_2-w)\\ \qquad (i=4,\ d_2+w\le z\le d_2+w+d_4)\ ,\end{cases} \tag{5}$$

$$H=[P_x^2+P_y^2+P_z^2]/2m_i^*-eV_a\quad (i=5,z>a)\ , \tag{6}$$

where $U_i(z)$ is the heterostructure potential, F_2, F_3, and F_4 are the electric-field strengths in regions II, III, and IV separately, and V_a is the total applied bias dropped across the structure. In the GaAs/Al_xGa_{1-x}As case, compared with the other terms in the Hamiltonian, the spin-magnetic-field interaction is neglected.

A. Eigenenergies and eigenwave functions of the Hamiltonian equation

In region I ($z<0$), the electron wave function is made of two plane waves incident onto and reflected from the structure

$$\Psi_I(x,y,z)=\exp(ik_xx)\exp(ik_yy)\times[A_1\exp(ik_z^1z)+B_1\exp(-ik_z^1z)]\ , \tag{7}$$

where $k_z^1=[2m^*(E-E_x-E_y^1)]^{1/2}/\hbar$ with E as the total energy of the electron and $E_x=\hbar^2k_x^2/2m_i^*$, and $E_y^1=\hbar^2k_y^2/2m_i^*$.

In regions II, III, and IV, the wave function of the electron is

$$\Psi_i(x,y,z)=\exp(ik_xx)\exp(ik_yy)\Phi_i(z)\ . \tag{8}$$

Now we can obtain the one-dimensional energy eigenvalue equation of the electron with effective mass

$$H_i(z)\Phi_i(z)=E_z\Phi_i(z)\ , \tag{9}$$

$$H_i(z)=-\frac{\hbar^2}{2m_i^*}\frac{\partial^2}{\partial z^2}+\frac{1}{2}m_i^*\omega_i^2(z-z_{0i})^2+C_i\ , \tag{10}$$

where $\omega_i=eB/m_i^*$, $z_{0i}=-\hbar k_y/eB+m_i^*F_i/eB^2$, and

$$C_i=\begin{cases}-(m_i^*/2B^2)(\hbar Bk_y/m_i^*-F_i)^2+\hbar^2k_y^2/2m_i^*+V_i(z) \quad (i=2)\\ -(m_i^*/2B^2)(\hbar Bk_y/m_i^*-F_i)^2+\hbar^2k_y^2/2m_i^*+V_i(z)+e(F_2-F_i)d_2 \quad (i=3)\\ -(m_i^*/2B^2)(\hbar Bk_y/m_i^*-F_i)^2+\hbar^2k_y^2/2m_i^*+V_i(z)+e(F_2-F_i)d_2+e(F_3-F_i)w \quad (i=4)\ .\end{cases} \tag{11}$$

When $C_i=$const, Eq. (10) reduces to the familiar harmonic-oscillator Hamiltonian, the solutions of which are equidistant Landau levels having the same energy $\hbar\omega_i(n+\frac{1}{2})$ $(n=0,1,2,\dots)$ for any k_y value. But in the presence of the magnetic field and a conduction-band offset, the translational invariance along z is broken and the eigenvalues of (10) depend on z_{0i}, the coordinate of the classical cyclotron orbit center.[20]

Now we define a new variable

$$\zeta=(m_i^* w_i/\hbar)^{1/2}(z-z_{0i}) \tag{12}$$

and the new function

$$\Phi_i(\zeta)=U(\zeta)\exp(-\zeta^2/2)\ . \tag{13}$$

Taking the Eqs. (10), (11), and (12) into Eq. (9), we come to the differential equation

$$\frac{d^2U(\zeta)}{d\zeta^2}-2\zeta\frac{dU(\zeta)}{d\zeta}+\lambda U(\zeta)=0\ , \tag{14}$$

where $\lambda=2(E_z-C_i)/(\hbar\omega_i)-1$. This is just a Hermitian equation with the general solution as

$$U(\zeta)=C_0U_0(\zeta)+C_1U_1(\zeta)\ , \tag{15}$$

where[21]

$$U_0(\zeta)=1+\frac{-\lambda}{2!}\zeta^2+\frac{-\lambda(4-\lambda)}{4!}\zeta^4+\cdots +\frac{(-\lambda)(4-\lambda)\cdots(4n-4-\lambda)}{(2n)!}\zeta^{2n}+\cdots\ , \tag{16}$$

$$U_1(\zeta)=\zeta+\frac{2-\lambda}{3!}\zeta^3+\frac{(2-\lambda)(6-\lambda)}{5!}\zeta^5+\cdots +\frac{(2-\lambda)(6-\lambda)\cdots(4n-2-\lambda)}{(2n+1)!}\zeta^{2n+1}+\cdots\ . \tag{17}$$

Then we can rewrite Eq. (8) as

$$\Psi_i(x,y,z)=\exp(ik_xx)\exp(ik_yy)[(A_i\Phi_i^1(\zeta)+B_i\Phi_i^2(\zeta)]\ , \tag{18}$$

where

$$\Phi_i^1(\zeta)=U_0(\zeta)\exp(-\zeta^2/2)\ , \tag{19}$$

$$\Phi_i^2(\zeta)=U_1(\zeta)\exp(-\zeta^2/2)\ . \tag{20}$$

The wave function of the electron in region V (that is, at the right electrode) is still the plane waves

$$\Psi_V(x,y,z)=\exp(ik_xx)\exp(ik_yy)\times[(A_5\exp(ik_z^rz)+B_5\exp(-ik_z^rz)]\ , \tag{21}$$

where

$$k_z^r=[2m_i^*(E-eV_a-E_x-E_y)]^{1/2}/\hbar\ ,$$

$$E_x=\hbar^2k_x^2/2m_i^*\ ,\quad E_y=\hbar^2k_y^2/2m_i^*\ .$$

B. The transmission coefficients $P(E,V,B,k_y)$

Imposing continuity of the wave function Ψ and its appropriately normalized derivative $(1/m_i^*)(d\Psi/dz)$ at the boundaries, we derive a matrix formula that relates the successive plane-wave coefficients A_5 and B_5 with A_1 and B_1, namely

$$\begin{bmatrix}A_1\\B_1\end{bmatrix}=\frac{1}{2ik_z^1}\begin{bmatrix}ik_z^1 & 1\\ ik_z^1 & -1\end{bmatrix}S_{(z)}\begin{bmatrix}\exp(ik_z^ra) & \exp(-ik_z^ra)\\ (m_4^*/m_5^*)ik_z^r\exp(ik_z^r) & -i(m_4^*/m_5^*)k_z^r\exp(-ik_z^ra)\end{bmatrix}\begin{bmatrix}A_5\\B_5\end{bmatrix}, \tag{22}$$

where

$$S(z)=S_2^*(z=0)S_2^{-1}(z=d_2)S_3^*(z=d_2)S_3^{-1}(z=d_2+w)S_4^*(z=d_2+w)S_4^{-1}(z=d_2+w+d_4)\ , \tag{23}$$

$$S_i(z)=\begin{bmatrix}\Phi_i^1(z) & \Phi_i^2(z)\\ d\Phi_i^1(z)/dz & d\Phi_i^2(z)/dz\end{bmatrix}, \tag{24}$$

$$S_i^*(z)=\begin{bmatrix}\Phi_i^1(z) & \Phi_i^2(z)\\ (m_{i-1}^*/m_i)(d\Phi_i^1(z)/dz) & (m_{i-1}^*/m_i^*)(d\Phi_i^2(z)/dz)\end{bmatrix}. \tag{25}$$

Setting $A_1=1$, $B_1=R$, $A_5=T$, $B_5=0$, and

$$S(z)=\begin{bmatrix}s_{11} & s_{12}\\ s_{21} & s_{22}\end{bmatrix}$$

in Eq. (22) which physically corresponds to an electron incident from the left-hand side of Fig. 1 and generates left-justified states, the transmission coefficient P is now defined as the ratio of the transmitted particle flux divided by incident particle flux, and depends on the incident electron energy E, the applied voltage V, and the magnetic-field strength B. This definition leads directly to the following simple expression:

$$P(E,V,B,K_y)$$
$$=4(k_z^l/k_z^r)\{[(k_z^l/k_z^r)s_{11}+(m_4^*/m_5^*)s_{22}]^2$$
$$+[s_{21}/k_z^r-(m_4^*/m_5^*)k_z^l s_{12}]^2\}^{-1}\ . \tag{26}$$

Here we like to point out that although we derive Eq. (26) from the GaAs/$Al_xGa_{1-x}As$ DBRTS, we can also expand Eq. (26) to the case of superlattices by just changing Eq. (23) as

$$S(z)=S_2^*(z=0)S_2^{-1}(z=d_2)S_3^*(z=d_2)$$
$$\times S_3^{-1}(z=d_2+w_1)$$
$$\times\cdots S_{2n}^{-1}(z=d_2+d_4+d_{2n}+\cdots$$
$$+w_1+w_2+\cdots w_{n-1})\ . \tag{27}$$

C. Tunneling current density $J(B,V)$

The tunneling current per area for a DBRTS, at a given applied bias V, can be calculated within the stationary-state (free-electron) model[17,21,22]

$$J=\int P(E_z,V,B)g(E_z,V)dE_z\ , \tag{28}$$

where $g(E_z,V)$ is the one-dimensional carrier-energy distribution function (CEDF) and expressed as

$$g(E_z,V)=\frac{em^*K_bT}{2\pi^2\hbar^3}\ln\frac{1+\exp[(E_f-E_z)/K_bT]}{1+\exp[(E_f-E_z-eV)/K_bT]}\ , \tag{29}$$

where $g(E_z,V)$ decreases with energy E_z and increases with temperature T for all energies monotonically.

III. RESULT AND DISCUSSION

Using Eq. (26) in Sec. II, we calculate transmission coefficients for four specific GaAs/$Al_xGa_{1-x}As$ devices. Device A (Refs. 17 and 18) has two 200-Å $Al_{0.24}Ga_{0.76}As$ barriers surrounding a 30-Å GaAs well, the whole width of the structure is larger, but the heights of barriers are lower. Device B (Ref. 23) has two 28-Å $Al_{0.3}Ga_{0.7}As$ barriers surrounding an 80-Å GaAs well. Device C (Ref. 22) has two 30-Å $Al_{0.8}Ga_{0.2}As$ barriers surrounding a 60-Å GaAs well. Both the widths of device B and device C are small, and their barrier heights are higher. Device D (Ref. 13) is an asymmetric heterostructure, with a 30-Å $Al_{0.5}Ga_{0.5}As$ barrier and a 40-Å $Al_{0.4}Ga_{0.6}As$ barrier surrounding a 60-Å GaAs well.

In Fig. 2, ln$P$ as functions of the energy E is presented at zero bias for device A, where $k_x=k_y=0$. The results reveal that for device A with much lower barriers and thicker width, the peak transmission coefficient P_m at resonance is almost equal to unity at $B=0$, and it will be far off unity when the magnetic field becomes a little stronger ($B=5$ T). But for devices B and C with higher barriers

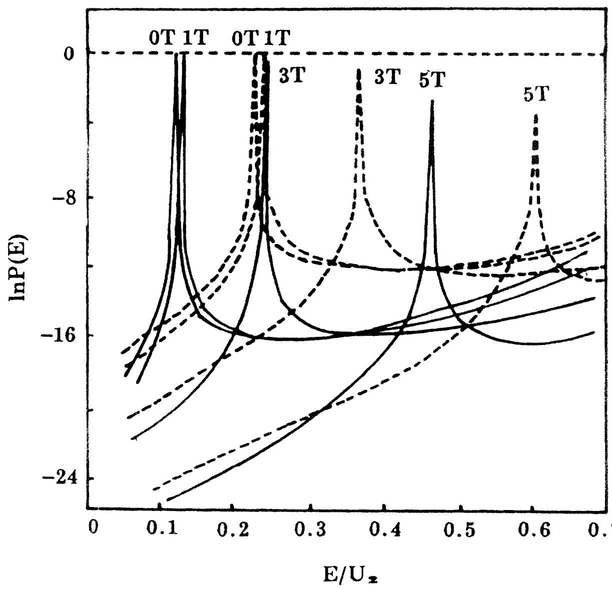

FIG. 2. Transmission coefficients vs energy for device A with no applied voltage. Four magnetic fields are considered, namely, 0, 1, 3, and 5 T. $k_x=k_y=0$. ——, $m_b^*=0.087m_e$, $m_w^*=0.067m_e$; – – –, $m_w^*=m_b^*=0.067m_e$.

and thinner width, as shown in Figs. 3 and 4, P_m at resonance is still nearly equal to unity for a large magnetic-field strength B and it will not be off unity until the magnetic field becomes much stronger. In Figs. 2 and 3 the dotted lines represented our results in which the same electron effective masses are taken inside the well and barriers. With the comparison of the dotted lines with the solid ones, it is shown that the mass effect influences

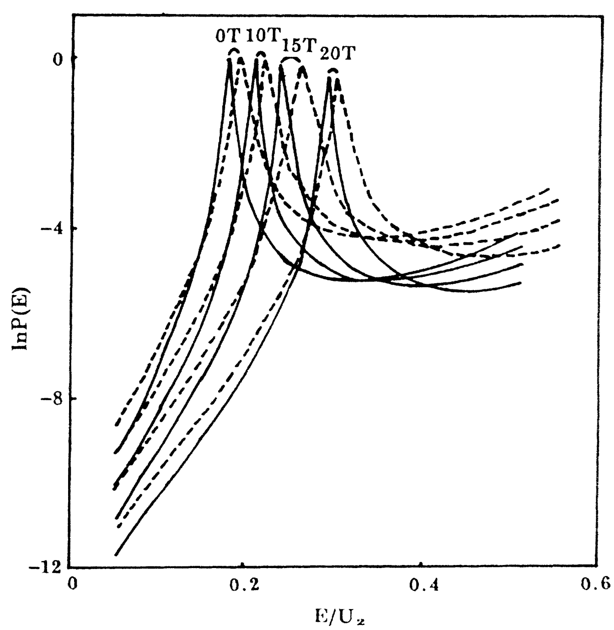

FIG. 3. Transmission coefficients vs energy for device B with no applied voltage. $B=0,10,15,20$ T. ——, $m_w^*=0.067m_e$, $m_b^*=0.0919m_e$; – – –, $m_w^*=m_b^*=0.067m_e$; $k_x=k_y=0$.

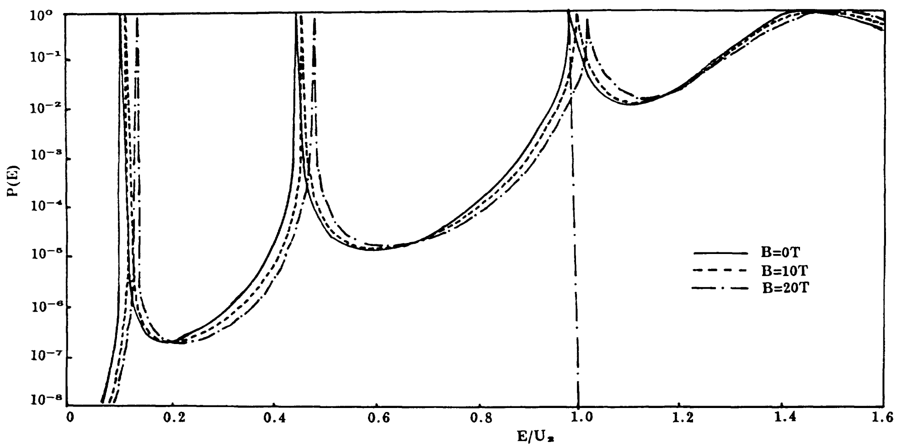

FIG. 4. Transmission coefficients vs energy for device C without applied voltage. $B=0,10,20$ T, $m_b^*=0.1334m_e$, $m_w^*=0.067m_e$, $k_x=k_y=0$. The transmission peaks in the quantum region are centered on 76.967 and 313.477 meV.

on transmission, in general, is more important, and will still affect the transport characteristics significantly.

In Fig. 4, for device C, we can see that sharp peaks occur at the resonant energies 76.967 and 313.477 meV in the quantum region, which are the energies of the ground state and first excited quasibound state in the well, respectively. These coincide with the results (77.135 and 313.61 meV) obtained by Turley and Teitsworth.[22] It is also found that the resonant peaks become narrow and shift to higher energies with increasing magnetic field.

It is well known that resonant tunneling[24] will occur if the incident energy E of particles is equal to a quasilocal level E_0 within the barriers. The value of P is maximum at resonance. When E is not equal to E_0, the value of P will decrease greatly. So the transmission coefficient has a sharp peak near $E=E_0$ and the thickness of the confining barriers mainly affects the width of the peak, which is related to the lifetime for the escape out of the well.[25] The results as shown in Figs. 2–4 can be easily interpreted as the following: at $B=0$, the potential in the structures is symmetric with respect to the center of the well, so the maximum of the transmission coefficient P is always equal to unity. However, the presence of magnetic fields will break such a symmetry of the effective potential. The degree of broken symmetry is determined by the magnetic-field strength and the parameters of DBRTS's. For DBRTS's with lower barriers and thicker width, the effective potential is strongly asymmetric even when the magnetic field B is very weak, so P_m decreases obviously with the increasing of the magnetic field B. But for devices B and C, even when the magnetic-field strength is very large, the symmetry of the effective potentials is not severely distorted due to the higher barriers and thinner width of the whole structures. So P_m is not far off unity until B becomes much larger. In order to verify our conclusions, we also calculate $P(E,V,B,k_y)$ on the asymmetric device D. In Fig. 5 the curve at $B=0$ for the asymmetric structure shows that P_m will not be equal to unity ($\ln P_m \sim -0.728\times10^{-1}$) and it decreases with increasing magnetic field because the symmetry of the effective potential is further broken by the presence of the magnetic fields.

Some of the above results are quite different qualitatively from those obtained by Ancilotto[17] and Cruz, Hernandez-Cabrera, and Aceituno.[18] Ancilotto[17] computed two linearly independent (numerical) solutions of the Schrödinger equation in the interval $[0,a]$ by using the WKB approximation. They matched the solutions with the plane-wave solutions and used the same electron effective masses inside the well and barriers. Cruz, Hernandez-Cabrera, and Aceituno[18] solved the one-dimensional effective-mass equation analytically by means of the confluent hypergeometric functions as envelope functions and calculated the transmission coefficients by using the transfer-matrix model. They presented their computed results only for device A, in which it is pointed out that the value $P(E)$ at resonance is not affected by the magnetic field (i.e., $P_m=1.0$ for any applied magnetic-field strength) and the resonant peak shifts slightly as the magnetic field strength increases. The overall shape of the transmission coefficient reflects the expected reduction in the current along the heterostructure axis (see Fig. 2 in Ref. 18). As in the above

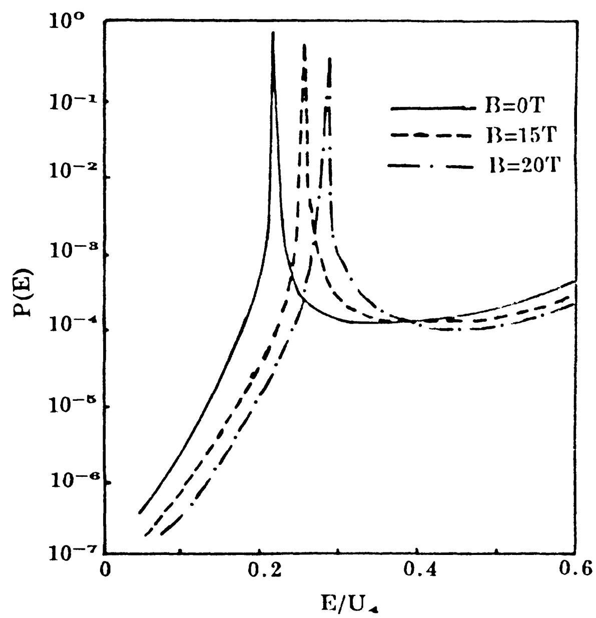

FIG. 5. Transmission coefficients vs energy for asymmetric device D with no applied voltage. $B=0,15,20$ T, $k_x=k_y=0$.

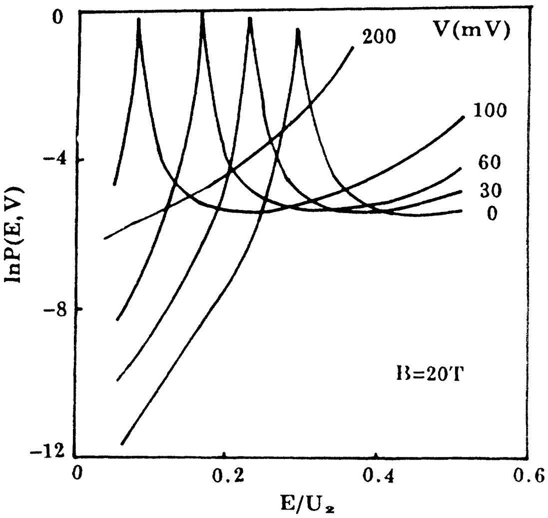

FIG. 6. Transmission coefficients vs energy for device B with $V=0$, 0.03, 0.06, 0.10, and 0.20 V at $B=20$ T, $k_x=k_y=0$.

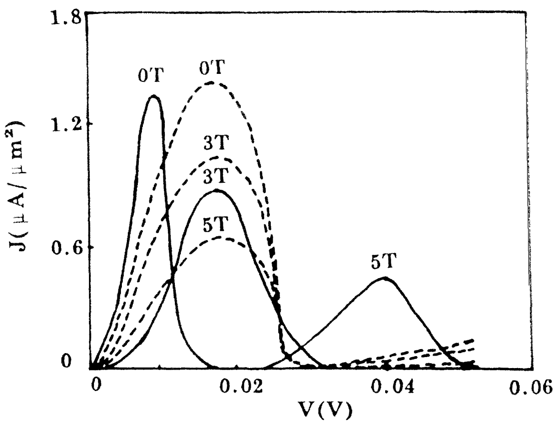

FIG. 7. Tunneling currents for device A. Three magnetic fields are considered, namely, 0, 3, and 5 T. ——, this work; — — —, from Ref. 17.

statements, our results for device A reveal that P_m at resonance is not always equal to unity and the resonant peak markedly shifts to higher energy when the magnetic-field strength B increases.

Figure 6 shows the variation of the transmission coefficient P (in logarithmic scale) versus the energy E of the incident particles for different applied bias on device B. We can see that when the magnetic field keeps constant, the peaks of $P(E,V,B,k_y)$ will shift to lower energy as the bias increases. At the outset P_m increases slightly and after it nearly reaches the unity value, P_m begins to decrease until the peak disappears. It is well known that under bias the quantum-energy levels in the well shift to lower energy and the higher the applied bias is, the lower the sublevel will be, so the peak shifts to lower energy with increasing bias. In the viewpoint of the symmetry, it is learned that the bias lifts the effective potential towards rightdown and the magnetic field lifts it towards rightup. As a result, with the magnetic field taken constant, the destruction on the effective potential symmetry due to the presence of the magnetic field is weakened by the increased bias, and, therefore, P_m will increase until P_m is nearly equal to unity. Then the symmetry of the effective potential is distorted severely again as the bias becomes very large, so at last P_m inversely decreases with increasing bias. When the sublevel in the well approaches energy lower than the conduction-band edge E_c, there is no electron that can resonant-tunnel through the device and no resonant peak occurs again.

The positions and amplitudes of the resonances observed in the $J(V)$ characteristics are slightly changed by the presence of a parallel magnetic field $\mathbf{B}_{\parallel}$.[3–7] This result can be understood classically since there is no Lorentz force component associated with the motion of an electron in the direction of the applied electric field. However, when the magnetic field is perpendicular to the tunneling current (i.e., $\mathbf{B}\perp\mathbf{J}$), the electronic motion in the quantum well is greatly modified. In contrast to the case for $\mathbf{B}\parallel\mathbf{J}$, the transverse field ($\mathbf{B}\perp\mathbf{J}$) attenuates the resonances in $J(V)$. In Fig. 7 the solid lines show the J-V characteristic of the DBRTS A (here taking $E_f=12$ meV and $T=4.2$ K), for several applied magnetic fields B. Compared with the WKB tunneling current per unit area under the magnetic field obtained by Ancillotto,[17] we obtain a sharp current peak as a function of applied voltage at $B=0$. Upon increasing the magnetic field, the resonance becomes weaker and shifts to higher voltages.

IV. SUMMARY AND CONCLUSIONS

In summary, the one-dimensional effective-mass equation is solved analytically by means of Hermitian functions as envelope functions under crossed magnetic and electric fields. Applying the transfer-matrix method, we calculate the transmission coefficients for electrons tunneling through several types of DBRTS's. The reasonable interpretations for all calculated results are presented in this paper. From a semiclassical point of view, due to the change in the momentum along the current direction induced by the Lorentz force, the effective potential of the DBRTS will increase with increasing magnetic-field strength. Subsequently, the transmission coefficients will decrease and the resonant peaks will become narrow and shift to high energy. From the view of the symmetry, due to the presence of the magnetic field and the electric field, the degrees to which the symmetry of the effective potential is destroyed in different DBRTS's are different, therefore, the peak transmission coefficient P_m is off unity in different degrees with increasing of magnetic field or the applied bias. The J-V characteristics of DBRTS's are also presented, in which owing to the change in the electron transverse momentum induced by the field, the peak markedly decreases and shifts to a high bias with increasing magnetic field.

It should be pointed out that for simplicity we neglect some effects such as space-charge effects, many-body interactions, phonon-scattering, etc., that may be significant in determining the J-V curves of real devices. The possible role of such effects depends sensitively on device parameters and should be considered in constructing a complete picture of resonant tunneling in double-barrier structures.

ACKNOWLEDGMENTS

We would like to thank Mr. Xiang-dong Zhang for useful and stimulating discussions. This project is supported by Hebei Province Science Foundation of China.

[1]R. Tsu and L. Esaki, Appl. Phys. Lett. **22**, 562 (1973); L. L. Chang, L. Esaki, and R. Tsu, *ibid.* **24**, 593 (1974).

[2]T. C. L. G. Sollner, W. D. Goadhue, P. E. Tannenwald, C. D. Parker, and D. D. Peck, Appl. Phys. Lett. **43**, 588 (1983).

[3]E. E. Mendez, L. Esaki, and W. I. Wang, Phys. Rev. B **33**, 2893 (1986).

[4]V. J. Goldman, D. C. Tsui, and J. E. Cunningham, Phys. Rev. B **35**, 9387 (1987).

[5]A. Zaslavsky, D. C. Tsui, M. Santos, and M. Shayegan, Phys. Rev. B **40**, 9829 (1989).

[6]M. L. Leadbeater, E. S. Alves, L. Eaves, M. Henini, O. H. Hughes, A. Celeste, J. C. Portal, G. Hill, and M. A. Pate, Phys. Rev. B **39**, 3438 (1989).

[7]Hou-zhi Zheng, Fu-hua Yang, and Zong-gui Chen, Phys. Rev. B **42**, 5270 (1990).

[8]R. A. Davies, D. J. Newson, T. G. Powell, M. J. Kelly, and H. W. Myron, Semicond. Sci. Technol. **2**, 61 (1987).

[9]M. L. Leadbeater, L. Eaves, P. E. Simmonds, G. A. Toombs, F. W. Skeard, P. A. Claxton, G. Hill, and M. A. Pate, Solid State Electron. **31**, 707 (1986).

[10]M. Helm, F. M. Perters, P. England, J. R. Hayes, and E. Colas, Phys. Rev. B **39**, 3427 (1989).

[11]P. England, J. R. Hages, M. Helm, J. P. Harbison, L. T. Florez, and S. J. Allen, Appl. Phys. Lett. **54**, 1469 (1989).

[12]M. L. Leadbeater, E. S. Alves, L. Eaves, M. Henini, O. H. Hughes, A. Celeste, J. C. Portal, G. Hill, and M. A. Pate, J. Phys. Condens. Matter **1**, 4865 (1989).

[13]A. Zaslavsky, Yuan P. Li, D. C. Tsui, M. Santos, and M. Shayegan, Phys. Rev. B **42**, 1374 (1990).

[14]T. Osoda, N. Minda, and L. Eaves, Solid State Commun. **81**, 119 (1992).

[15]R. C. Potter and A. A. Lakhani, Appl. Phys. Lett. **52**, 1349 (1988).

[16]E. S. Alves, M. L. Heighes, A. Celeste, and J. C. Portal, Superlatt. Microstruct. **5**, 527 (1989).

[17]F. Ancilotto, J. Phys. C **21**, 4677 (1988).

[18]H. Cruz, A. Hernandez-Cabrera, and P. Aceituno, J. Phys. Condens. Matter **2**, 8053 (1990).

[19]H. C. Casey and M. B. Panich, *Heterostructure Lasers* (Academic, New York, 1978), Pt. A, Chap. 4.

[20]G. Belle, J. C. Maan, and G. Weimann, Solid State Commun. **56**, 65 (1985).

[21]Kongmiao Liang, *Method of Mathematics and Physics* (People's Educational Press, Beijing, 1960).

[22]P. J. Turley and S. W. Teitsworth, Phys. Rev. B **44**, 3199 (1991).

[23]K. M. Hung and G. Y. Wu, Phys. Rev. B **45**, 3461 (1991).

[24]B. Ricco and M. Ya. Azkel, Phys. Rev. B **29**, 1970 (1984).

[25]F. Anicilotto, A. Solloni, and E. Tosattio, Phys. Rev. B **40**, 3729 (1989).